Hidvégi Norbert Tibor (Orcid ID: 0000-0003-3665-2724)
Gulyás Andrea (Orcid ID: 0000-0001-6978-1341)

Ultrasound, as a hypomethylating agent, remodels DNA methylation and alters mRNA transcription in winter wheat (*Triticum aestivum* L.) seedlings

Norbert Hidvégi[1,†,*], Andrea Gulyás[1, †], Judit Dobránszki[1]

[1]Centre for Agricultural Genomics and Biotechnology, Faculty of the Agricultural and Food Science and Environmental Management, University of Debrecen, Nyíregyháza, Hungary

[†]These authors contributed equally

*Corresponding author: hidvegi.norbert@agr.unideb.hu

Abstract

Any treatment that affects seed germination and seedling development is of paramount importance from an agricultural point of view since they are critical prerequisites for successful crop production. In present study, we have examined the after-effect of ultrasonication (at 30 kHz, 70 W for 5 minutes) of winter wheat (*Triticum aestivum* L. cv. SE15) seeds on the early seedling growth and development, and accompanying changes in the DNA methylation and transcriptomic pattern in 7-day-old seedlings. We used mRNA-sequencing and Whole Genome Bisulfite Sequencing (WGBS) to identify significantly differentially expressed genes (DEGs), significantly differently methylated regions (DMRs) and genes (DMGs). Ultrasonication of seeds did not alter the germination rate but increased both the length and weight of roots and shoots of 7-day-old seedlings significantly by 23- 68% and 16-28%, respectively. Analysing the expression intensity of 107,891 genes, significantly differentially expressed sequences related mainly to starch biosynthesis, IAA biosynthesis, photosynthesis and TCA cycle pathways. The same pathways were also affected by DNA-methylation changes. DNA hypomethylation occurred in the global methylation profile after ultrasound treatment altering the accessibility of some genes for transcription. Transcriptomic changes suggested alterations in the crosstalk between IAA and sucrose signalling, enhancement of growth processes, and increased activity of nuclear transcription factor stimulating the transcription of genes having CCAAT motif in the promoter. In the present first whole genome level study, we have identified seed ultrasonication as a priming technique that can act as a hypomethylating agent and thereby is able to modify the mRNA transcription allowing enhanced seedling growth.

Keywords: enhanced growth, seed ultrasonication, DNA hypomethylation, transcriptional changes

Introduction

Nowadays, agriculture focuses on applications and technologies that stimulate seed germination, plant growth and development, and thus yields, and at the same time, they have little or no negative impact on the environment. Targeted use of physical environmental cues can be one of the solutions to improve plant growth and yield (Telewski 2006, Trakselyte-Rupsiene et al. 2021). Acoustic waves, like sound and ultrasound (US) are forms of physical environmental cues that are ubiquitous in nature and act on plants as abiotic stressors (Teixeira da Silva and Dobránszki 2014).

Ultrasound, defined as acoustic waves with a frequency greater than 20 kHz, can affect both the structure and function of macromolecules, as discovered already in the last century (Timonin 1966, Yaldagard et al. 2008). Low frequency US waves (10-60 kHz) are able to interact with the cells and tissues of plants and have biological effects on plants by modifying the growth and development. The effects on living cells and tissues are caused by mechanical and thermal processes (Rokhina et al. 2009, Teixeira da Silva and Dobránszki 2014).

Ultrasonic stimulation of seed germination has been described in the model plant *Arabidopsis thaliana* (Col-0 ecotype) (López-Ribera and Vicient 2017) and in many crops of agricultural importance, including sunflower (*Helianthus annuus* L.) (Hebling and Da Silva 1995), rice (*Oryza sativa* L.) (Mo et al. 2020), and barley (*Hordeum vulgare* L.) (Yaldagard et al. 2008). Recent studies on seed ultrasonication of different crops revealed its enhancing effects on germination, growth and development and its activating effect on the antioxidant system of plants. Germination of either naturally aged or artificially deteriorated *Arabidopsis* seeds were improved by ultrasonication (at 45 kHz, 0.028 W m^{-3}, 24°C, for 30 s; USC-1400 ultrasonic bath) after cold imbibition of the seeds (López-Ribera and Vicient 2017). The authors assumed that the increased germination might be due to the higher number of pores in the seed coat as they observed by scanning electron microscopy. Yaldagard et al. (2008) ultrasonicated (at 20 kHz, 200%, 60% and 100% of 460 W, for 5, 10 and 15 min) the barley seeds in an ultrasonicator, where the seeds were put into tap water for the duration of the treatment (60 g seeds / 80 ml tap water). A reduced germination time and as a result of an increase in the activity of α-amylase were detected after ultrasonication of the barley seeds. The optimal treatment was ultrasonication with 460 W for 15 min. The germination time reduced (from 7 to 4-5 days), and the α-amylase activity increased (from 177.74 to 190.431 U/g malt) as the US power and the exposure time increased. As they hypothesized, the larger porosity of barley seeds caused by the ultrasonication enhanced the water diffusion, and the enhanced fluidity of cell walls caused by the nutrient mobilization from endosperm may be responsible for the stimulation of the germination process. When the seeds of rice (*Oryza sativa* L. cvs. Nongxiang and Meixiangzhan) were ultrasonicated (20-40 kHz, for 30 min) using an ultrasonic seed processor (JD-1L, Guangzhou, China) and then sown in the field, the dry biomass, the net photosynthetic rate in the leaves, the grain yield, the panicle number, the grain number per panicle and the percentage of filled grains have increased. Ultrasonication increased the activity of SOD (superoxide dismutase) and POD (peroxidase) in the leaves; SOD activity increased in response to US by up to 84.9%, while the POD activity increased by up to 121.5%, depending on the variety, and the developmental stage. The 2-acetyl-1-pyrroline content in grains increased by up to 50.2-88.1%

depending on the variety, as well as increased the proline content from 10.1% to 59.9% in Meixiangzhan and from 2.7% to 122% in Nongxiang (Mo et al. 2020).

A microarray-based study by Wilson et al. (2005) was the first detailed examination of the transcriptome of winter wheat (*Triticum aestivum* L. cv. Mercial) embryo during maturation and germination. mRNA accumulation related to amino acid biosynthesis, cell division and formation of new cells, respiration and energy production, mobilization of stored proteins and abscisic acid (ABA) signalling were observed 1 and 2 days after germination. However, the study demonstrated that the majority of transcripts necessary for growth and development after initiation of germination was already accumulated in the mature and dormant embryo cells, but they were not translated. Transcripts of translation activation factors had accumulated, however, directly before and during germination, which led to the translation of pre-existing transcripts. Examination showed that there are a very small number of new transcripts at the beginning of germination. An increase in the level of a transcript encoding a protein similar to the indole acetic acid-alanine (IAA-Ala) hydrolase of rice, and a concomitant decrease in the level of another transcript encoding a protein similar to IAA-Ala resistance protein 1 of *Arabidopsis thaliana* was observed, which indicates the role of free auxin in the germination (elongation of coleoptile).

Detailed dynamic transcriptomic analysis (Yu et al. 2014) revealed that the first 48 h of germination of Chinese bread wheat consists of three distinct phases, each regulated by gene networks. In the first 12 h after imbibition, the genes related to the degradation of small-molecule sucrose were activated, while in the next 12 h, genes responsible for the metabolism of major nutrients (carbohydrates, proteins and lipids), moreover, genes related to the cell wall metabolism were up-regulated. The expression intensity of metabolic genes increased from 24 h to 36 h after imbibition, and by the 48 h after imbibition genes responsible for photosynthesis were up-regulated. The study identified the functional groups with involved genes and the main interactions between important genes. In cereals, the level of hydrogen peroxide (H_2O_2) can promote seed germination, hence abiotic stressors may play a role in stimulating germination. According to the comparative transcriptomic study of Yu et al. (2016), the ratio of ABA and H_2O_2 plays a regulating role in the expression of genes related to seed germination. Nevertheless, there is no study on transcriptomic and epigenetic changes of seedlings in response to seed ultrasonication.

In the present study, we have examined whether ultrasonication applied as a pre-sowing treatment directly before the germination of winter wheat seeds affects germination and early seedling development. Furthermore, we also sought to answer the question of what changes in gene expression and DNA methylation of seedlings were associated with ultrasonication of seeds.

Materials and methods

Plant material and ultrasonic treatment of winter wheat seeds

In the present experiments, the germination of a breeding line of winter wheat (*Triticum aestivum* L. cv. SE15) was investigated. The water content of the seeds was 13.6%. Half of the seeds (100 seeds) were ultrasonicated before germination at 30 kHz, 70 W for 5 min. The seeds were placed into open Petri dishes 4 cm from the ultrasound head. The parameters of the ultrasound treatment have been optimized previously in preliminary experiments. The other half of the seeds (100 seeds) served as control and were non-ultrasonicated. Thereafter, winter wheat seeds were germinated at 20°C in darkness for a week, in accordance with the Hungarian standard of MSZ 6354-3:2008 describing the determination of germination.

Sampling and statistical evaluation of seedling growth and development

Seedling samples were collected 7 days after germination. Three independent biological samples were collected both from the control and the ultrasonicated plant material and stored at -80°C until DNA and RNA analysis.

Lengths, fresh weights of shoots and roots, and the number of roots per 7-day-old seedlings were measured. Data were analysed by Independent Samples T-test at $P < 0.05$ using SPSS for Windows software (SPSS®, version 21.0).

Isolation of total RNA and preparation of libraries for mRNA sequencing

Total RNA was isolated from each wheat sample (Control and Ultrasound) in three biological replicates using the Direct-zol™ kit (Zymo Research) and TRIzol reagent according to the manufacturer's methodology. After purifying total RNA, three quality control (QC) methods were used: (1) preliminary quantification with an Implen N50 spectrophotometer (Implen,); (2) agarose gel electrophoresis to assess RNA degradation and potential contamination; and (3) Agilent Bioanalyzer 2100 system (Agilent). Novogene, a genome sequencing company, performed mRNA capturing, cDNA library preparation, and sequencing after the three-step QC. mRNA is produced using the company's methodology (rRNA-depleted RNA-seq). The oligo(dT) beads were used to enrich mRNA from the two wheat samples. Plant Ribo-Zero rRNA removal kit (Illumina) was used to remove rRNA according to the manufacturer's procedure. For mRNA-seq library preparation from wheat samples, the Illumina TruSeq Stranded mRNA kit (Illumina) was used. To quantify and optimize library concentration, Qubit 2.0 fluorometric quantitation (Thermo Fischer Scientific), Agilent Bioanalyzer 2100 (Agilent), and AriaMX qPCR (Agilent) were used. The NovaSeq 6000 sequencer (Illumina) was used to sequence the two qualifying libraries. The libraries were sequenced with 150 bp paired-end reads and 20 M reads per sample.

mRNA-seq datasets bioinformatic pipeline

FastQC v0.11.9 (https://github.com/s-andrews/FastQC/releases) was used to QC FASTQ files.

TrimGalore v0.6.7 (https://github.com/FelixKrueger/TrimGalore/releases) was used to do adapter and quality trimming using default parameters. To avoid sequence biases caused by oligo(dT) and random hexamer primers, 10 bp were removed from the 5′ end of the readings (Hansen et al. 2010). STAR v2.7.10a (Dobin et al. 2013) was used to align reads to the *Triticum aestivum* (iwgsc_refseqv1.0: https://plants.ensembl.org/Triticum_aestivum/Info/Index) reference genome (Consortium et al. 2018) using default configuration which we downloaded from the Ensembl Plant database.

Known splice sites were identified using the STAR script to create a splice sites file from a GFF annotation file. STAR generated aligned reads in BAM files, which were then imported into SeqMonk v1.48.1 (https://github.com/s-andrews/SeqMonk/releases) with a mapping quality of 60 to select only uniquely aligned reads. The resulting quantified values were log2 transformed readings per million input reads (LFC: logarithmic fold change). To filter the statistically differentially expressed genes, the edgeR (Empirical Analysis of Digital Gene Expression Data in R (Robinson et al. 2010, McCarthy et al. 2012)) and DESeq2 (Differential gene expression analysis based on the negative binomial distribution (Love et al. 2014)) statistical analyses were performed on the aligned reads (DEGs).

Sample preparation for Whole Genome Bisulfite Sequencing (WGBS)

Following the manufacturer's instructions, DNA was extracted and purified from both wheat samples using a NucleoSpin plant II DNA extraction kit (Macherey-Nagel). Two biological replicates were used. According to the user manual, bisulfite was used to detect cytosine methylation status using the NEBNext Enzymatic Methyl-seq Kit (New England Biolabs) and 100 ng of genomic DNA. The WGBS was carried out on an Illumina NovaSeq 6000 (Illumina) using 150 bp paired-end (PE) reads with 10x whole genome coverage, and differential methylation analysis was carried out across the two treatment groups.

Extraction of methylation and whole genome bisulfite sequencing assembly

FastQC v0.11.9 (https://github.com/s-andrews/FastQC) was used to evaluate the quality of DNA reads generated from WGBS sequencing. TrimGalore v0.6.7 (https://github.com/FelixKrueger/TrimGalore/releases) was used to do adapter and quality trimming using default parameters with cutadapt v3.4 (Martin 2011). Following sequence quality control, an average of 170 Gb/sample of Illumina PE reads (approximate sequencing depth = 10x) were assembled separately using Bowtie v2.4.5 (Langmead et al. 2009) based on the *Triticum aestivum* (iwgsc refseqv1.0: https://plants.ensembl.org/Triticum_aestivum/Info/Index) genome data (Consortium et al. 2018), Bismark v0.23.1 was used to perform DNA methylation analysis and gene clustering analysis to analyse methylation patterns (Krueger and Andrews 2011).

SeqMonk v1.48.1 (https://github.com/s-andrews/SeqMonk) was used to perform differential methylation, statistical analysis in percentage, DNA methylation distribution plots, and gene clustering on sets of 100 CpGs, CHGs and CHHs. Based on the DNA methylation levels, unreplicated differential methylation was done using a $\chi2$ test ($P < 0.05$) and replicated differential methylation was done using edgeR ($P< 0.05$), as significantly differentially methylated regions (DMRs) over upstream (-3000 bp upstream of the transcription start site (TSS) of the gene), overlapping (gene body as an entire gene from TSS to the end of transcription) and downstream (+3000 bp downstream of the TSS of the gene) regions. We identified exactly overlapping regions on the gene body which has been unreplicated ($\chi2$ test) and replicated differential methylation (edgeR) with a 25% absolute difference cut-off from the control, as significantly differentially methylated genes (DMGs).

The $\chi2$ test and edgeR results in CpG, CHG and CHH contexts, were visualized using a SeqMonk-generated MA plot (Bland-Altman plot), in which the differences in measurements between any of the two samples in all permutations were assessed by transforming the data using SeqMonk onto M (log ratio) and A (mean average) scales and plotting these values (Bland and Altman 1999); quantitation trend plot (QTP) to visualize methylation percentage of DMRs over upstream, overlapping and downstream regions; bean plot to visualize the distribution of DNA methylation levels of DMRs; BoxWhisker plot (box plot) to visualize the distribution of DNA methylation levels of DMGs with median, minimum and maximum values; and correlation matrix to visualize pairwise correlation values between control and ultrasonicated samples based on Pearson correlation coefficient values (https://www.bioinformatics.babraham.ac.uk/projects/seqmonk/Help/).

DEGs, DMRs and DMGs functional annotation

OmicsBox v2.1 (Götz et al. 2008) was used to annotate the DEGs, DMRs and DMGs with functional annotation and an analytic pipeline. We used BlastX-fast with a minimum E-value score of 1.0E-06, based on the NCBI nucleotide database (filter on *Triticum aestivum* L.). After Blast, the blast impacts were mapped and annotated using GO mapping, with an annotation cut-off threshold set to 55 and GO level weighting set to 5. After GO mapping, InterProScan was performed and merged to annotation based on different databases. The biological, molecular, and cellular pathways connected to DEGs, DMRs and DMGs were determined using KEGG v101.0 (Kyoto Encyclopedia of Genes and Genomes) pathway maps (Kanehisa et al. 2021) and Plant Reactome v22 (Naithani et al. 2020) with EggNOG database v5.0.0 (Huerta-Cepas et al. 2019), as an additional functional annotation.

Results

Effects of ultrasonication on seedling growth and development

Ultrasonication of winter wheat seeds affected the growth and development of 7-day-old seedlings. Except for the number of roots per seedling, which was not affected, all parameters were significantly increased in response to ultrasonication of the seeds (Figure 1B). The length of shoots and roots of seedlings (Figure 1A) increased by 68% and 23%, respectively, in response to seed ultrasonication, while the increase in the shoot and root weight were 28% and 16%, respectively.

Identification of DEGs in the whole genome

Comparing the ultrasonicated seedlings (US1) with control (non-ultrasonicated) seedlings (K1), MA plot (Bland-Altman plot) and hierarchical cluster analysis (heatmap) were applied for DEGs (Figure 2A, B). We found two different clusters of DEGs between US1 and K1, which included 18 DEGs. We identified TraesCS5B02G353200, TraesCS5A02G350600 and TraesCS1D02G411300 genes in the first cluster; TraesCS6D2G088800, TraesCS5A02G454300, TraesCS6A02G093700, TraesCS5D02G464700, TraesCS5A02G454200, TraesCS1B02G317500, TraesCS1D02G375100, TraesCS6A02G350300, TraesCS5D02G227000, TraesCS5D02G227500, TraesCS2B02G510200, TraesCS1D02G027300, TraesCS7D02G057200, TraesCS1B02G433300 and TraesCS4A02G081000 in the second cluster (Figure 2A). We observed 3 down-regulated (TraesCS5D02G227000, TraesCS5D02G227500 and TraesCS6A02G350300) and 15 up-regulated DEGs (TraesCS1B02G317500, TraesCS1B02G433300, TraesCS1D02G027300, TraesCS1D02G375100, TraesCS1D02G411300, TraesCS2B02G510200, TraesCS4A02G081000, TraesCS5A02G350600, TraesCS5A02G454200, TraesCS5A02G454300, TraesCS5B02G353200, TraesCS5D02G464700, TraesCS6A02G093700, TraesCS6D02G088800 and TraesCS7D02G057200) in the whole genome (Figure 2B, Table 1).

DEG analysis of biological processes, cellular components and molecular functions

The expression intensity of 107,891 genes of hexaploid *Triticum aestivum* L. cv. SE15 was assessed using RNA-seq analysis to identify the biological processes, cellular components and molecular functions affected in response to seed ultrasonication. The involvement of biological processes, cellular components and molecular functions are presented in Figure S1. A total of 25 biological processes were significantly affected, of which 13 were up-regulated and 12 were down-regulated. Relative highest percentages of upregulated biological processes were responses to light stimuli (21.27%), cellular protein modification (19.15%), precursor metabolites and energy production (19.15%), and photosynthesis (19.15%). Down-regulated biological processes accounted for the same relative percentage (8.33% each).

Among the cellular components, nucleus and cytosol were hardly affected (in 3.45% of each), but three locations (thylakoid, membrane and chloroplast) were largely affected and up-regulated (31.03% each). Down-regulation was observed only in relation to the chloroplast thylakoid membrane (100%).

Considering the molecular functions, a total of 6 molecular functions (DNA-binding, DNA-binding transcription factor activity, transferase activity, enzyme regulator activity, hydrolase activity and protein binding) were significantly up-regulated in equal proportions (16.67% each). No down-regulation in molecular function was detected.

Up- or down-regulated metabolic and cellular functions in response to seed ultrasonication

When comparing control (non-ultrasonicated) and ultrasonicated samples and if the results of both bioinformatics analyzes (edgeR and DESeq2) were taken into account, it can be stated with certainty that 18 sequences were significantly differentially expressed, either up-or down-regulated (Table 1.).

12 out of 18 differentially expressed genes (DEGs) were mapped for four metabolic pathways using Plant Reactome and KEGG, and all were up-regulated by ultrasonication. Nine DEGs related to starch synthase, catalyze the conversion of ADP-D-glucose into (1,4-α-D-glucosyl)(n+1)) in starch biosynthesis. Two DEGs were related to SCS dimer operating in the mitochondrial matrix and convert Succinyl-CoA to Succinate in the TCA cycle. However, one of those 2 DEGs (TraesCS5A02G350600) is hypothesized that operates as a photosynthesis antenna protein (Lhcb1), as part of the light-harvesting chlorophyll protein complex (LHC). One DEG (TraesCS4A02G081000) was identified, which belongs to the amidase family of proteins. It converts indole-3-acetamide to indole-3-acetate in IAA biosynthesis.

The function of the remaining 6 DEGs could be determined based on the NCBI. Of the 6 DEGs, three were up-, and three were down-regulated. One DEG encoded xyloglucan endotransglucosylase/hydrolase protein 9-like isoform X2 was up-regulated. This protein plays a role in the cleavage and re-ligation of xyloglucan polymers. DEG related to subtilisin-chymotrypsin inhibitor-2B-like protein, which participates in response to wounding, was also up-regulated. The last DEG, which was up-regulated is responsible for uncharacterized isomerase BH0283-like that has an isomerase activity and participates in biosynthetic processes. Two out of three down-regulated DEGs related to low molecular mass early light-inducible protein HV90, a chloroplastic-like protein likely involved in the pigment integration into mature pigment-protein complexes. The third down-regulated DEG encoded a cold-shock protein (CS120-like, dehydrin).

Changes in DNA methylation pattern in response to seed ultrasonication

Comparing the DNA methylation level of ultrasonicated and control samples, MA plot, quantitation trend plot (QTP), bean plot, correlation matrix and box plot analysis were applied to determine and compare the DMGs. We identified and observed the methylation level of DMGs in CpG, CHG and CHH contexts. Based on the MA plots, we found increased or decreased DNA methylation levels in all three contexts (Figure 3A, B, C). We identified DMGs between 10% and 90%, 10% and 80%, 10% and 40% as an average of DNA methylation levels in CpG, CHG and CHH contexts, respectively. The differences of DNA methylation level between ultrasonicated and control samples were between -20% and -70%, 20% and 80%; -23% and -50%, 24% and 70%; -24% and -58%, 22% and 57% in CpG, CHG and CHH contexts, respectively (Figure 3A, B, C).

The QTP were made on the whole genome based on the methylation level of DMRs in CpG, CHG and CHH contexts. When comparing the methylation level of DMRs in the CpG context, the DNA methylation level of upstream and downstream regions was higher than in the gene body at up from -500 bp and up from +500 bp from TSS of the genes. In the CpG context, the DNA methylation level of DMRs was higher in K1 than in US1 (Figure 4A). The methylation level of DMRs in the CHG context was higher upstream and downstream than in the gene body. In the CHG context, the DNA methylation level of DMRs was higher in ultrasonicated samples than in control ones (Figure 5A). The methylation level of DMRs in the CHH context was higher in the upstream region than in the downstream region and gene body. In the CHH context, the DNA methylation level of DMRs was higher in ultrasonicated samples than in control ones at up from -1000 bp and up from +1000 bp from TSS of the genes (Figure 6A).

Distributions of global DNA methylation levels of DMRs in CpG, CHG and CHH contexts were visualised with a bean plot (Figure 4B, 5B, 6B). In the CpG context, the distributions of DNA methylation levels show that the vast majority of the control and ultrasonicated genomes were highly methylated (>90%), with only a small subset staying unmethylated (Figure 4B). In the CHG context, the distributions of DNA methylation levels show that both genomes were methylated mostly more than 50%, with only a small DMRs staying unmethylated (Figure 5B), while in the CHH context both genomes generally were methylated to an extent less than 20% (Figure 6B).

Based on the Pearson correlation of DMGs, a correlation matrix in the CpG, CHG and CHH contexts was made between control and ultrasonicated samples. Pearson correlation coefficients were 0.98, 0.58 and 0.63 in the CpG, CHG and CHH contexts, respectively (Figure 4C, 5C, 6C).

Box plots were made to visualize the distribution of DNA methylation levels of DMGs in the CpG, CHG and CHH contexts (Figure 4D, 5D, 6D). In the CpG context, the distribution of DNA methylation levels of DMGs was between 35% and 75%, 20% and 65%, with 60% and 40% median in control and ultrasonicated samples, respectively (Figure 4D). In the CHG context, the distribution of DNA methylation levels of DMGs was between 10% and 35%, 5% and 30%, with 20% and 15% median in control and ultrasonicated samples, respectively (Figure 5D), while in the CHH context was between 5% and 20%, 1% and 6% with 12% and 3% median in control and ultrasonicated samples, respectively (Figure 6D).

A Venn diagram was made to visualize the distribution of DMGs in the CpG, CHG and CHH contexts. 228, 149 and 80 DMGs were identified in the CpG, CHG and CHH contexts, while 14 DMGs were identified in both the CpG and CHG contexts and no DMGs were found in all three contexts (Figure 7).

DMG analysis of biological processes, cellular components and molecular functions

The changes in DNA methylation of DMGs involved in biological processes, molecular functions and cellular components were mapped by the GO database in OmicsBox (Table 2, Figures S2, S3 and S4). DMGs are presented in Table 2 according to the contexts and regions in which they were methylated differentially in 7-day-old seedlings. A total of 912 sites in biological process, molecular function and cellular component were identified as either hypo- or hypermethylated after seed ultrasonication considering all contexts. The GO annotations were found in 228, 149 and 80 DMGs, in CpG, CHG and CHH contexts, respectively. Most differentially methylated genes identified (460 genes) related to biological processes and CpG context. It was 50.4% in DMGs related to biological processes while 21.2% and 28.4% in DMGs related to molecular functions and cellular components, respectively. It was 45.2% in DMGs related to the CpG context while 37.2% and 17.6% in DMGs related to CHG and CHH contexts, respectively. Considering all regions (upstream, overlapping, downstream) and all contexts (CpG, CHG and CHH) of affected DMGs, hypomethylation was significant, 1.8-fold higher than hypermethylation.

Pathway analysis of DMGs based on the Plant Reactome and KEGG

While determining the pathways related to differentially methylated genes (DMGs) by Plant Reactome and KEGG maps, a total of 268 sites were identified in CpG, CHG or CHH contexts, which were differentially methylated upstream, overlapping or downstream regions after ultrasonication of seeds (Supplementary Table 1). The hypomethylation detected in mapped DMGs was almost twice (1.88-fold) higher than the hypermethylation observed in those DMGs. The least methylation change (51) occurred in the CHH context; by comparison, 1.6-fold more methylation changes could be detected in the CHG context (83) and 2.6-fold more in the CpG context (134). In upstream regions, hypermethylation could be detected in 14-14 DMGs in CpG and CHG contexts and 3 DMGs in CHH context, while hypomethylation occurred in 22, 10, and 14 DMGs in CpG, CHG and CHH contexts, respectively. In the downstream regions, hypomethylation (in 17, 12, and 18 DMGs in the context of CpG, CHG, and CHH, respectively) was 2.5-fold higher than hypermethylation (in 9, 5, and 5 DMGs in the context of CpG, CHG, and CHH, respectively). Most methylation changes could be detected in the overlapping regions, and hypomethylation (in 46, 26, and 10 DMGs in the context of CpG, CHG, and CHH, respectively) was approximately twice as high as hypermethylation (in 26, 16, and 1 DMGs in the context of CpG, CHG, and CHH, respectively) but to varying degrees depending on contexts.

The changes in DNA-methylation of DMGs involved in pathways mapped by the Plant Reactome and KEGG are shown in Table 3. DMGs are presented in the table (Table 3) according to the contexts and regions in which they were methylated differentially in 7-day-old seedlings after seed ultrasonication compared to the control, i.e. non-ultrasonicated one. A total of 456 sites in the 268 DMGs were identified as either hypo- or hypermethylated after seed ultrasonication considering all contexts and regions. Differentially methylated regions were detected in at least one of the CpG, CHG or CHH contexts of DMGs encoding proteins that participate in pathways of cellular processes, energy and precursor metabolism, growth and developmental processes, metabolism and regulation, response to biotic and abiotic stimuli and stresses and circadian rhythm. Most differentially methylated regions identified (330 regions, 72% of all differentially methylated regions) are related to the metabolism and regulation pathways, and mainly to amino acid metabolism (78 regions), hormone signalling, transport and metabolism (64 regions), cofactor biosynthesis (55 regions) and carbohydrate metabolism (45 regions). Considering all regions (upstream, overlapping, downstream) and all contexts (CpG, CHG and CHH) of affected DMGs, hypomethylation was significantly higher than hypermethylation. It was 72% in DMGs related to all pathways of metabolism and regulation, while 69%, 64%, 78%, and 71% in DMGs related to amino acid metabolism, hormone signalling, transport and metabolism, cofactor biosynthesis, and carbohydrate metabolism, respectively. Differentially methylated regions related to cellular processes and energy and precursor metabolism, growth and developmental processes, and response to abiotic stimuli and stresses occurred only in 9%, 8% and 8% of all differentially methylated regions, respectively.

Discussion

Seed ultrasonication, as a presowing treatment, had an after-effect on 7-day-old seedlings of winter wheat. Although ultrasound treatment has been reported to stimulate seed germination in many plant species (Hebling and Da Silva 1995, Yaldagard et al. 2008, Goussous et al. 2010, López-Ribera and Vicient 2017, Mo et al. 2020), we found no difference in the germination percentage of control and ultrasonicated seeds, 7 days after germination. This is probably since the germination rate of the control seeds were already high (99%). Ultrasonication of winter wheat seeds immediately before germination, however, enhanced the growth and development of seedlings. Both the length and fresh weight of shoots and roots of 7-day-old seedlings were significantly increased (Figure 1).

The after-effects of seed ultrasonication were also detectable in the different mRNA expression patterns of control and ultrasonicated seedlings. RNA-seq revealed transcriptomic changes connected to the biological processes, primarily responses to light stimuli, cellular protein modification, precursor metabolites and energy production and photosynthesis, and they mainly affected the cellular components of thylakoid, membrane and chloroplast. Molecular functions connected to the transcription and its regulation were up-regulated (Supplementary Figure 1). Up-regulation of DEGs related to starch biosynthesis, IAA biosynthesis, photosynthesis and TCA cycle pathways (Table 1) is consistent with the observations of changes in growth parameters after ultrasonication. IAA priming of cotton (*Gossypium hirsutum* L.) seeds improved the root and shoot length and biomass of the two true leafy seedlings, promoted photosynthesis and altered the sucrose metabolism (Zhao et al. 2020). The crosstalk between IAA and sucrose signalling may play a prominent role in affecting seedling growth and development via regulating cell expansion and cell division (Wang and Ruan 2013). Increased expression intensities of DEGs encoding sucrose synthase and the DEG related to IAA biosynthesis suggest that affecting these signalling pathways may be one of the reasons behind the enhancement of the seedling growth observed in response to seed ultrasonication (Mishra et al. 2022). Similarly, the increased expression of xyloglucan endotransglucosylase/hydrolase protein 9-like isoform X2 (Table 1) indicates the enhancement of growth processes, due to its role in the internodal elongation of plant cells which is characteristic of the cell wall structure in growing plant tissues (Chano et al. 2017). In addition, DEG related to IAA biosynthesis has an assumed nuclear transcription factor Y subunit C-2-like function by which it can stimulate the transcription of different genes having CCAAT motif in their promoters (Gusmaroli et al. 2001). In the case of the three down-regulated DEGs (Table 1, Figure 2A, B), TraesCS5D02G22700 and TraesCS5D02G227500 genes' function is unknown. When the *Aegilops tauschii* (Tausch's goatgrass) genome was resequenced and reannotated, and then compared with the *Triticum aestivum* genome, these genes were identified as orthologous genes (Zhou et al. 2021), which were similar LFC values (-4.22 and -4.23) detected in our present study (Table 1). TraesCS6A02G350300 gene encodes dehydrin (DHN) protein (*TaDHN10-A* gene) (Hao et al. 2022). *The taDHN10-A* gene was up-regulated with high TPM (Transcripts Per Kilobase Million) values under drought and cold stresses (Wang et al. 2014, Hao et al. 2022). DHN genes respond to biotic and abiotic stress on a high scale of gene expression intensity (up-, or down-regulation), depending on the stress type (Hao et al. 2022). The DHN gene was reported earlier to be down-regulated under ultrasonication treatment (Oda et al. 2021). Similarly, we also identified down-regulating of the DHN gene in our study.

The global methylation profiles of control and ultrasonicated samples were different to each other. The global DNA methylation level was lower in the ultrasonicated sample than in the control sample (Figure 8B). It was 89.3%, 55.9% and 1.6% for CpG, CHG and CHH contexts, respectively, in the control sample, while 87.0%, 52.7% and 1.5% for CpG, CHG and CHH contexts, respectively, in the ultrasonicated sample (Figure 3A, B, C). This hypomethylation state was observed in both DMRs (Figure 4B, 5B, 6B) and DMGs (Figure 4D, 5D, 6D). Similar hypomethylation was identified in *Brachypodium distachyon* (Borowska et al. 2011) and *Paeonia suffruticosa* Andr. (Zhang et al. 2020) under 5-azacytidine treatment. Based on the Pearson correlation coefficients results, we have identified that ultrasound treatment may cause higher DNA methylation level changes in the CHG and CHH contexts than in CpG contexts (Figure 4C, 5C, 6C and Figure 8A, 8B). We observed hypomethylation in different GO annotations, especially in biological processes in CpG, CHG and CHH contexts. The DNA methylation level changes were higher in the CpG context of DMGs (Table 2, Figure 4C), which included 228, 149 and 80 DMGs in the CpG, CHG and CHH contexts, respectively (Figure 7), while DNA methylation level changes were higher in the CHG context of DMRs (Figure 5C). Ultrasound treatment may act as a hypomethylating agent, which causes significant demethylation of genomic DNA.

Up-regulated DEGs were identified during the RNA expression analysis in the four main pathways, such as IAA biosynthesis VI (via indole-3-acetamide), the TCA cycle (plant), starch biosynthesis and photosynthesis. DNA methylation changes associated with these pathways could also be detected (Supplementary Table 1). Four DMGs affecting IAA biosynthesis pathways in plants were identified. They were hypomethylated in downstream regions either in CHG or CpG contexts, in the upstream region in CHH contexts, and hypermethylated in upstream regions in the CpG context, separately. The DMG hypomethylated downstream in the CpG context was related to the IAA biosynthesis pathway VI (via indole-3-acetamide), similarly to DEG, which has been shown to be upregulated in RNA expression analysis. Four genes related to the TCA cycle were differentially methylated, all in the overlapping regions of the genes, one of those was hypermethylated in the CHG context, while the other 3 were hypomethylated in CHH, CHG and CpG contexts, respectively. All detected DMGs encoded the same enzyme catalysing the Succinyl-CoA to Succinate conversion. In the RNA analysis, 2 DEGs were detected to be up-regulated that encodes the same enzyme (Table 3). Two DMGs could be identified that were either hyper-, or hypomethylated, respectively, in overlapping regions of DMGs, both in the CHG context, which was related to starch biosynthesis. Both DMGs encoded phosphoglucomutase catalysing interconversion of glucose-6-phosphate and glucose-1-phosphate. However, the upregulated 9 DEGs detected in RNA expression analysis encode a starch synthase involved in a later step in the starch biosynthetic pathway. Thereby, no direct correlation between the DNA-methylation and RNA expression of genes participating in the starch biosynthesis pathway could be observed. Similarly, no direct correlation between the DNA-methylation and RNA transcription of the affected genes could be observed when the photosynthesis pathway was examined. Five DMGs related to photosynthesis were identified, all were hypomethylated in either CHG, or CpG contexts (Supplementary Table 1). Although the expression intensities of those DMGs did not change, the up-regulation of DEGs related to photosynthesis was detected (Table 1). In the two latter cases, in starch biosynthesis and photosynthesis, additional detailed expression and regulation analysis of genes, including identification of transcriptional regulators, involved in the pathways is necessary for young seedlings similarly as it was studied in the wheat seeds (Gu et al. 2021). Such further analysis can help to accurately understand these indirect relationships between the state of DNA methylation and gene transcription. Furthermore, it should also be taken into account that DNA methylation is only one component of the epigenetic mechanisms that may regulate gene transcription (Chang et al. 2020, Guarino et al. 2022).

Seeds are essential in building the production capacity of a crop plant. Seed germination is the vital period of a plant establishment, and rapid germination and seedling emergence are critical factors for successful plant establishment (Harris et al. 1999). In recent years, ultrasonication has been applied as an efficient technique for breaking seed dormancy, improving seed germination (Aladjadjiyan 2011, Mihaylova et al. 2021), and enhancing drought stress tolerance (Ran et al. 2015). The molecular genetic and epigenetic mechanisms of action of ultrasound on seeds and its after-effects on seedlings are still unclear. This study provides the first, whole genome-level insight into the epigenetic and transcriptomic landscape of young wheat seedlings after seed ultrasonication. Ultrasound treatment has been identified in our present study as a potential priming technique that can modify the global DNA methylation level and may act as a hypomethylating agent. The accessibility of genes for transcription can be altered by epigenetic modifications. In this study, we observed the global and region-specific changes in DNA methylation levels by ultrasound that altered the transcription of some genes (Figure 9). Chromatin remodelling is one of the epigenetic modifications regulating transcription in response to stresses. However, DNA methylation is only one epigenetic modification of chromatin remodelling, and the latter is only one among epigenetic modifications. Other epigenetic changes, e.g. histone modifications, small RNAs, long non-coding RNAs, etc., and their cross-talk also regulate transcription (Chang et al. 2020, Guarino et al. 2022). Therefore, further studies are necessary for determining other gene expression regulatory mechanisms in wheat seedlings in response to ultrasound treatment. Moreover, our results presented here raise the additional question, which is of importance from the agricultural cultivation point of view, whether there is an after-effect, and if so, what kind of after-effect the seed ultrasonication has on the development of the plant in the field, i.e. on biomass, flowering, seed yield, etc. and what about their molecular background.

Author Contribution Statement

JD conceived and designed the experiments and conducted the germination trials. NH and AG conducted the molecular works and the bioinformatics analyses. JD, NH and AG analysed the data and co-wrote all versions of the paper. JD, NH and AG take responsibility for the content of the paper.

Conflict of Interest Statement

Authors declare no conflicts of interest.

Acknowledgement

Project No. TKP2021-EGA-20 (Biotechnology) has been implemented with the support provided from the National Research, Development and Innovation Fund of Hungary, financed under the TKP2021-EGA funding scheme.

Data availability

The raw Illumina mRNA-seq datasets were submitted to NCBI and the processed data were deposited under GEO ID GSE200377 and BioProject ID PRJNA824414 for six samples: GSM6032332, GSM6032333, GSM6032334, GSM6032335, GSM6032336 and GSM6032337. The raw Illumina and MGI WGBS datasets were submitted to NCBI and the processed data were deposited under GEO ID GSE202558 and BioProject PRJNA836562 for four samples: GSM6124435, GSM6124436, GSM6124437 and GSM6124438.

References

Aladjadjiyan, A. (2011) Ultrasonic stimulation of the development of lentils and wheat seedlings. *Romanian journal of biophysics* 21(3), 179-187

Bland, J.M. & Altman, D.G. (1999) Measuring agreement in method comparison studies. *Statistical methods in medical research* 8(2), 135-160 https://doi.org/10.1191/096228099673819272

Borowska, N., Idziak, D. & Hasterok, R. (2011) DNA methylation patterns of Brachypodium distachyon chromosomes and their alteration by 5-azacytidine treatment. *Chromosome research* 19(8), 955-967 https://doi.org/10.1007/s10577-011-9243-2

Chang, Y.N., Zhu, C., Jiang, J., Zhang, H., Zhu, J.K. & Duan, C.G. (2020) Epigenetic regulation in plant abiotic stress responses. *Journal of integrative plant biology* 62(5), 563-580 https://doi.org/10.1111/jipb.12901

Chano, V., de Heredia, U.L., Collada, C. & Soto, Á. (2017) Transcriptomic analysis of juvenile wood formation during the growing season in Pinus canariensis. *Holzforschung* 71(12), 919-937 https://doi.org/10.1515/hf-2017-0014

Consortium, I.W.G.S., Appels, R., Eversole, K., Stein, N., Feuillet, C., Keller, B., Rogers, J., Pozniak, C.J., Choulet, F. & Distelfeld, A. (2018) Shifting the limits in wheat research and breeding using a fully annotated reference genome. *Science* 361(6403), eaar7191

Dobin, A., Davis, C.A., Schlesinger, F., Drenkow, J., Zaleski, C., Jha, S., Batut, P., Chaisson, M. & Gingeras, T.R. (2013) STAR: ultrafast universal RNA-seq aligner. *Bioinformatics* 29(1), 15-21 https://doi.org/10.1093/bioinformatics/bts635

Goussous, S., Samarah, N., Alqudah, A. & Othman, M. (2010) Enhancing seed germination of four crop species using an ultrasonic technique. *Experimental Agriculture* 46(2), 231-242 https://doi.org/10.1017/S0014479709991062

Götz, S., García-Gómez, J.M., Terol, J., Williams, T.D., Nagaraj, S.H., Nueda, M.J., Robles, M., Talón, M., Dopazo, J. & Conesa, A. (2008) High-throughput functional annotation and data mining with the Blast2GO suite. *Nucleic acids research* 36(10), 3420-3435 https://doi.org/10.1093/nar/gkn176

Gu, Y., Han, S., Chen, L., Mu, J., Duan, L., Li, Y., Yan, Y. & Li, X. (2021) Expression and regulation of genes involved in the reserve starch biosynthesis pathway in hexaploid wheat (Triticum aestivum L.). *The Crop Journal* 9(2), 440-455 https://doi.org/10.1016/j.cj.2020.08.002

Guarino, F., Cicatelli, A., Castiglione, S., Agius, D.R., Orhun, G.E., Fragkostefanakis, S., Leclercq, J., Dobránszki, J., Kaiserli, E. & Lieberman-Lazarovich, M. (2022) An epigenetic alphabet of crop adaptation to climate change. *Frontiers in Genetics* 13 https://doi.org/10.3389/fgene.2022.818727

Gusmaroli, G., Tonelli, C. & Mantovani, R. (2001) Regulation of the CCAAT-binding NF-Y subunits in Arabidopsis thaliana. *Gene* 264(2), 173-185 https://doi.org/10.1016/S0378-1119(01)00323-7

Hansen, K.D., Brenner, S.E. & Dudoit, S. (2010) Biases in Illumina transcriptome sequencing caused by random hexamer priming. *Nucleic acids research* 38(12), e131-e131 https://doi.org/10.1093/nar/gkq224

Hao, Y., Hao, M., Cui, Y., Kong, L. & Wang, H. (2022) Genome-wide survey of the dehydrin genes in bread wheat (*Triticum aestivum* L.) and its relatives: identification, evolution and expression profiling under various abiotic stresses. *BMC Genomics* 23(1), 73 https://doi.org/10.1186/s12864-022-08317-x

Harris, D., Joshi, A., Khan, P., Gothkar, P. & Sodhi, P. (1999) On-farm seed priming in semi-arid agriculture: development and evaluation in maize, rice and chickpea in India using participatory methods. *Experimental Agriculture* 35(1), 15-29 https://doi.org/10.1017/S0014479799001027

Hebling, S. & Da Silva, W. (1995) Effects of low intensity ultrasound on the germination of corn seeds (*Zea mays* L.) under different water availabilities. *Scientia Agricola* 52, 514-520 https://doi.org/10.1590/S0103-90161995000300017

Huerta-Cepas, J., Szklarczyk, D., Heller, D., Hernández-Plaza, A., Forslund, S.K., Cook, H., Mende, D.R., Letunic, I., Rattei, T. & Jensen, L.J. (2019) eggNOG 5.0: a hierarchical, functionally and phylogenetically annotated orthology resource based on 5090 organisms and 2502 viruses. *Nucleic acids research* 47(D1), D309-D314 https://doi.org/10.1093/nar/gky1085

Kanehisa, M., Furumichi, M., Sato, Y., Ishiguro-Watanabe, M. & Tanabe, M. (2021) KEGG: integrating viruses and cellular organisms. *Nucleic acids research* 49(D1), D545-D551 https://doi.org/10.1093/nar/gkaa970

Krueger, F. & Andrews, S.R. (2011) Bismark: a flexible aligner and methylation caller for Bisulfite-Seq applications. *bioinformatics* 27(11), 1571-1572 https://doi.org/10.1093/bioinformatics/btr167

Langmead, B., Trapnell, C., Pop, M. & Salzberg, S.L. (2009) Ultrafast and memory-efficient alignment of short DNA sequences to the human genome. *Genome biology* 10(3), 1-10 https://doi.org/10.1186/gb-2009-10-3-r25

López-Ribera, I. & Vicient, C.M. (2017) Use of ultrasonication to increase germination rates of Arabidopsis seeds. *Plant Methods* 13(1), 1-6 https://doi.org/10.1186/s13007-017-0182-6

Love, M.I., Huber, W. & Anders, S. (2014) Moderated estimation of fold change and dispersion for RNA-seq data with DESeq2. *Genome biology* 15(12), 1-21 https://doi.org/10.1186/s13059-014-0550-8

Martin, M. (2011) Cutadapt removes adapter sequences from high-throughput sequencing reads. *EMBnet journal* 17(1), 10-12 https://doi.org/10.14806/ej.17.1.200

McCarthy, D.J., Chen, Y. & Smyth, G.K. (2012) Differential expression analysis of multifactor RNA-Seq experiments with respect to biological variation. *Nucleic acids research* 40(10), 4288-4297 https://doi.org/10.1093/nar/gks042

Mihaylova, E., Marcheva, M. & Peruhov, N. (2021) Ultrasound seed treatment for organic farming. *Bulgarian Journal of Agricultural Science* 27, 1

Mishra, B.S., Sharma, M. & Laxmi, A. (2022) Role of sugar and auxin crosstalk in plant growth and development. *Physiologia Plantarum* 174(1), e13546 https://doi.org/10.1111/ppl.13546

Mo, Z., Liu, Q., Xie, W., Ashraf, U., Abrar, M., Pan, S., Duan, M., Tian, H., Wang, S. & Tang, X. (2020) Ultrasonic seed treatment and Cu application modulate photosynthesis, grain quality, and Cu concentrations in aromatic rice. *Photosynthetica* 58(3), 682-691 https://doi.org/10.32615/ps.2020.009

Naithani, S., Gupta, P., Preece, J., D'Eustachio, P., Elser, J.L., Garg, P., Dikeman, D.A., Kiff, J., Cook, J. & Olson, A. (2020) Plant Reactome: a knowledgebase and resource for comparative pathway analysis. *Nucleic acids research* 48(D1), D1093-D1103 https://doi.org/10.1093/nar/gkz996

Oda, S., Sakaguchi, M., Yang, X., Liu, Q., Iwasaki, K. & Nishibayashi, K. (2021) Ultrasonic treatment suppresses ethylene signaling and prolongs the freshness of spinach. *Food Chem (Oxf)* 2, 100026 https://doi.org/10.1016/j.fochms.2021.100026

Ran, H., Yang, L. & Cao, Y. (2015) Ultrasound on seedling growth of wheat under drought stress effects. *Agricultural Sciences* 6(07), 670 https://doi.org/10.4236/as.2015.67064

Robinson, M.D., McCarthy, D.J. & Smyth, G.K. (2010) edgeR: a Bioconductor package for differential expression analysis of digital gene expression data. *Bioinformatics* 26(1), 139-140 https://doi.org/10.1093/bioinformatics/btp616

Rokhina, E.V., Lens, P. & Virkutyte, J. (2009) Low-frequency ultrasound in biotechnology: state of the art. *Trends in biotechnology* 27(5), 298-306 https://doi.org/10.1016/j.tibtech.2009.02.001

Teixeira da Silva, J.A. & Dobránszki, J. (2014) Sonication and ultrasound: impact on plant growth and development. *Plant Cell, Tissue and Organ Culture (PCTOC)* 117(2), 131-143 https://doi.org/10.1007/s11240-014-0429-0

Telewski, F.W. (2006) A unified hypothesis of mechanoperception in plants. *American journal of botany* 93(10), 1466-1476 https://doi.org/10.3732/ajb.93.10.1466

Timonin, M. (1966) Effect of ultrasound on the germination of white spruce and jack pine seeds. *Canadian Journal of Botany* 44(1), 113-115 https://doi.org/10.1139/b66-017

Trakselyte-Rupsiene, K., Juodeikiene, G., Cernauskas, D., Bartkiene, E., Klupsaite, D., Zadeike, D., Bendoraitiene, J., Damasius, J., Ignatavicius, J. & Sikorskaite-Gudziuniene, S. (2021) Integration of Ultrasound into the Development of Plant-Based Protein Hydrolysate and Its Bio-Stimulatory Effect for Growth of Wheat Grain Seedlings In Vivo. *Plants* 10(7), 1319 https://doi.org/10.3390/plants10071319

Wang, L. & Ruan, Y.-L. (2013) Regulation of cell division and expansion by sugar and auxin signaling. *Frontiers in plant science* 4, 163 https://doi.org/10.3389/fpls.2013.00163

Wang, Y., Xu, H., Zhu, H., Tao, Y., Zhang, G., Zhang, L., Zhang, C., Zhang, Z. & Ma, Z. (2014) Classification and expression diversification of wheat dehydrin genes. *Plant Sci* 214, 113-120 https://doi.org/10.1016/j.plantsci.2013.10.005

Wilson, I.D., Barker, G.L., Lu, C., Coghill, J.A., Beswick, R.W., Lenton, J.R. & Edwards, K.J. (2005) Alteration of the embryo transcriptome of hexaploid winter wheat (Triticum aestivum cv. Mercia) during maturation and germination. *Functional & integrative genomics* 5(3), 144-154 https://doi.org/10.1007/s10142-005-0137-2

Yaldagard, M., Mortazavi, S.A. & Tabatabaie, F. (2008) Influence of ultrasonic stimulation on the germination of barley seed and its alpha-amylase activity. *African Journal of Biotechnology* 7(14) https://doi.org/10.1002/j.2050-0416.2008.tb00300.x

Yu, Y., Guo, G., Lv, D., Hu, Y., Li, J., Li, X. & Yan, Y. (2014) Transcriptome analysis during seed germination of elite Chinese bread wheat cultivar Jimai 20. *BMC plant biology* 14(1), 1-19 https://doi.org/10.1186/1471-2229-14-20

Yu, Y., Zhen, S., Wang, S., Wang, Y., Cao, H., Zhang, Y., Li, J. & Yan, Y. (2016) Comparative transcriptome analysis of wheat embryo and endosperm responses to ABA and H2O2 stresses during seed germination. *BMC genomics* 17(1), 1-18 https://doi.org/10.1186/s12864-016-2416-9

Zhang, Y., Si, F., Wang, Y., Liu, C., Zhang, T., Yuan, Y. & Gai, S. (2020) Application of 5-azacytidine induces DNA hypomethylation and accelerates dormancy release in buds of tree peony. *Plant Physiol Biochem* 147, 91-100 https://doi.org/10.1016/j.plaphy.2019.12.010

Zhao, T., Deng, X., Xiao, Q., Han, Y., Zhu, S. & Chen, J. (2020) IAA priming improves the germination and seedling growth in cotton (Gossypium hirsutum L.) via regulating the endogenous phytohormones and enhancing the sucrose metabolism. *Industrial Crops and Products* 155, 112788 https://doi.org/10.1016/j.indcrop.2020.112788

Zhou, Y., Bai, S., Li, H., Sun, G., Zhang, D., Ma, F., Zhao, X., Nie, F., Li, J. & Chen, L. (2021) Introgressing the Aegilops tauschii genome into wheat as a basis for cereal improvement. *Nature Plants* 7(6), 774-786 https://doi.org/10.1038/s41477-021-00934-w

Table 1. Significantly up- or down-regulated DEGs and related metabolic and cellular functions. Negative values indicate down-regulation; positive values indicate up-regulation in response to the ultrasonication of winter wheat seeds

Table 2. Distribution of DMGs in upstream, overlapping and downstream regions based on the GO annotation results.

Table 3. Participation of the DMGs in different pathways based on Plant Reactome and KEGG mapping. DMGs are presented according to the contexts and regions in which they were methylated differentially in 7-day-old seedlings after seed ultrasonication. Numbers mean the number of sequences involved; ↑ indicates hypermethylation while ↓ indicates hypomethylation compared to non-ultrasonicated samples. Note: A sequence can be involved in multiple pathways and a sequence may occur more than once in the table if it has been methylated differently in multiple contexts or regions.

Figure 1. Morphological parameters of 7-day-old winter wheat seedlings after exposure to ultrasound treatment (A). Shoot and root weights of 7-week-old seedlings mean the average fresh weights of them (mg), root number means the average number of roots per seedling. The length of roots and shoots was measured in mm per seedling. *: indicates the significant differences at $P < 0.05$ according to the Independent Samples T-test (B).

Figure 2. Heatmap (A) and MA plot (B) of DEGs between control (K1) and ultrasonicated (US1) samples. On the MA plot, the x-axis represents the average quantitated LFC (logarithmic fold change) values, while y-axis shows the differences between them.

Figure 3. MA plot of DMGs between control (K1) and ultrasonicated (US1) samples in CpG (A), CHG (B) and CHH (C) contexts. The x-axis represents the average quantitated LFC (logarithmic fold change) values, while y-axis shows the differences between them.

Figure 4. Profile of DMRs in CpG context (A) in upstream, overlapping and downstream from the TSS (transcription starting site) of gene. The x-axis represents the relative distance over gene, while the y-axis shows the DNA methylation level in percentage. Distribution profile of DMRs in CpG context on bean plot (B) and distribution profile of DMGs in CpG context on box plot (D). The y-axis represents the DNA methylation level in percentage. Correlation matrix based on the DMGs in CpG context in the control (K1) and ultrasonicated (US1) samples (C).

Figure 5. Profile of DMRs in CHG context (A) in upstream, overlapping and downstream from the TSS (transcription starting site) of gene. The x-axis represents the relative distance over gene, while the y-axis shows the DNA methylation level in percentage. Distribution profile of DMRs in CHG context on bean plot (B) and distribution profile of DMGs in CHG context on box plot (D). The y-axis represents the DNA methylation level in percentage. Correlation matrix based on the DMGs in CHG context in the control (K1) and ultrasonicated (US1) samples (C).

Figure 6. Profile of DMRs in CHH context (A) in upstream, overlapping and downstream from the TSS (transcription starting site) of gene. The x-axis represents the relative distance over gene, while the y-axis shows the DNA methylation level in percentage. Distribution profile of DMRs in CHH context on bean plot (B) and distribution profile of DMGs in CHH context on box plot (D). The y-axis represents the DNA methylation level in percentage. Correlation matrix based on the DMGs in CHH context in the control (K1) and ultrasonicated (US1) samples (C).

Figure 7. Venn diagram about distribution of CpG, CHG and CHH contexts based on the DMGs numbers.

Figure 8. Correlation between wheat gene expression and methylation. (A) Diagram of RNA expression (B) DNA methylation. (A) The outer layers indicate the reference genome of wheat. The first inner layers indicate differentially expressed transcripts in the control. The second inner layers indicate the expressed transcripts of the ultrasound-treated (US) plant and the third layers indicate the common significantly differentially expressed genes (DEG) found when expression intensities of both samples were compared. (B) The outer layers indicate the reference genome of wheat. The first inner layers (the horizontal lines) indicate significantly differently methylated genes (DMG) in the CpG context. The second inner layer indicates the CHG context, while the third inner layer indicates the CHH context.

Figure 9. Schematic roadmap of how seed ultrasonication affects gene transcription in young seedling and thereby their growth and development due to the DNA methylation re-modelling effect of ultrasound.

Supplementary Table 1. Pathway analysis of DMGs based on the KEGG and Plant Reactome databases.

Supplementary Figure 1. Gene annotations of DEGs based on the GO annotation results.

Supplementary Figure 2. Gene annotations of DMGs in CpG context based on the GO annotation results.

Supplementary Figure 3. Gene annotations of DMGs in CHG context based on the GO annotation results.

Supplementary Figure 4. Gene annotations of DMGs in CHH context based on the GO annotation results.

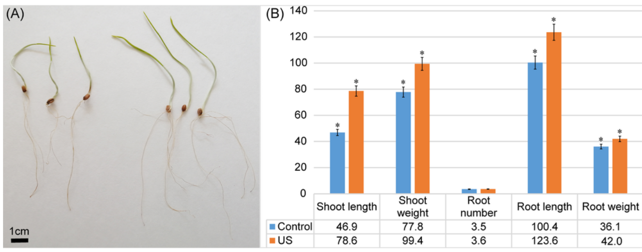

PPL_13777_Figure_1.tif

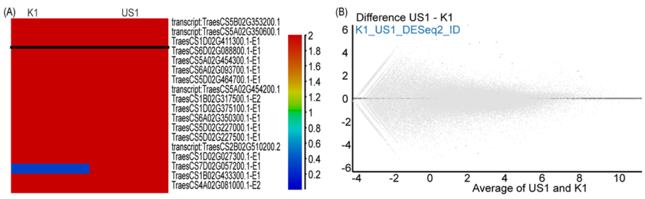

PPL_13777_Figure_2.tif

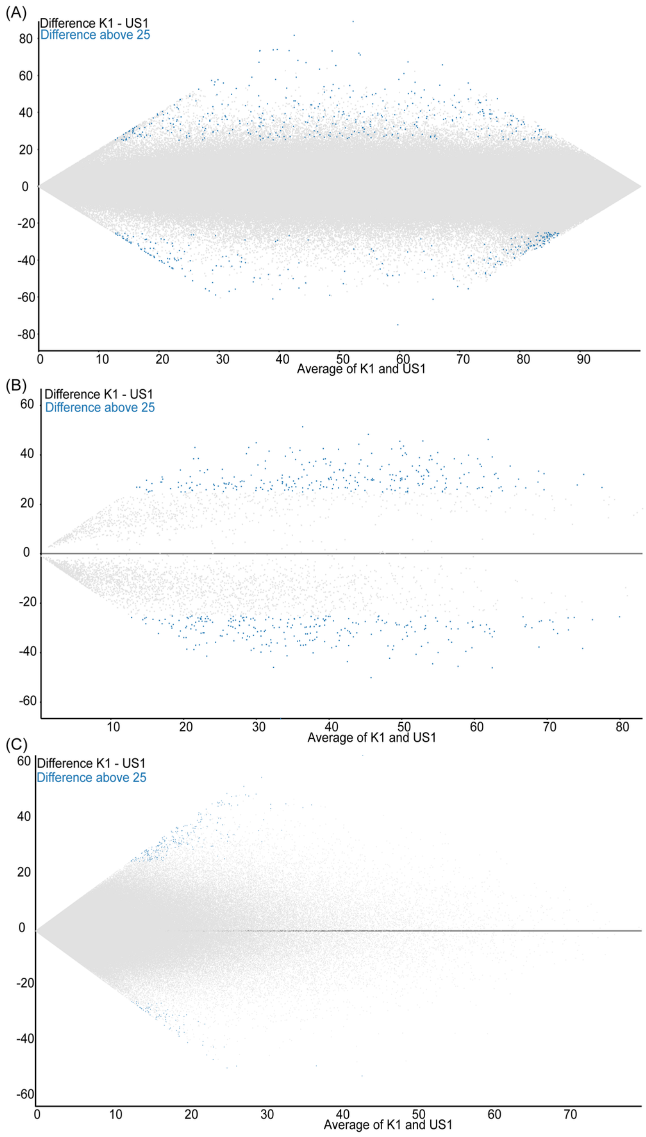

PPL_13777_Figure_3.tif

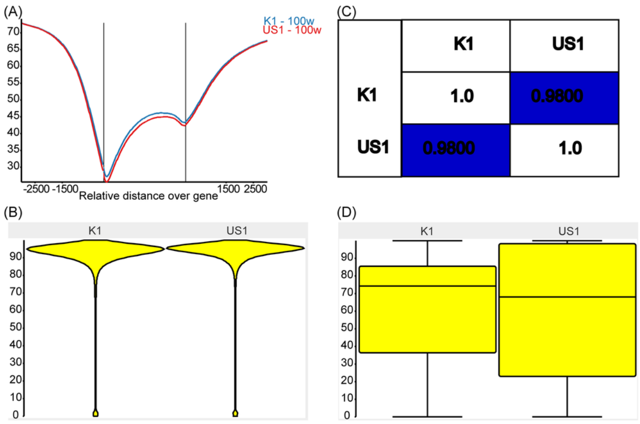

PPL_13777_Figure_4.tif

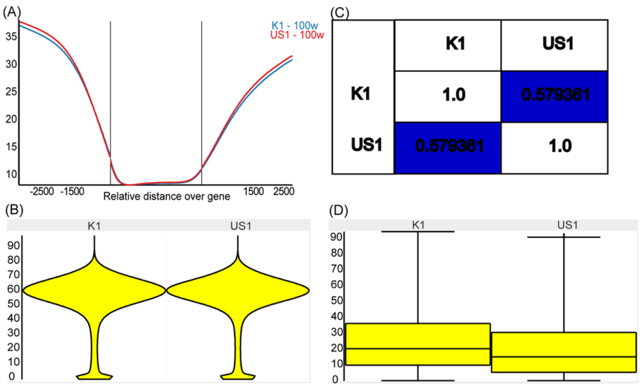

PPL_13777_Figure_5.tif

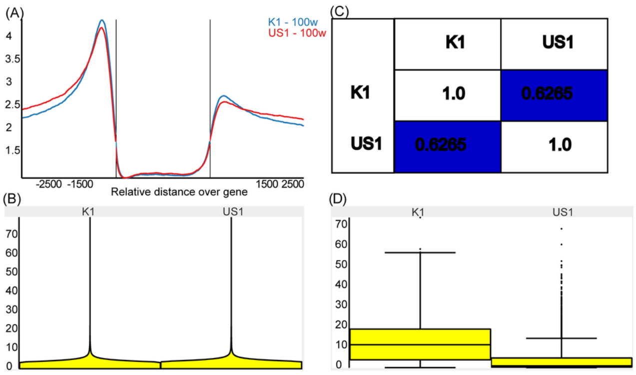

PPL_13777_Figure_6.tif

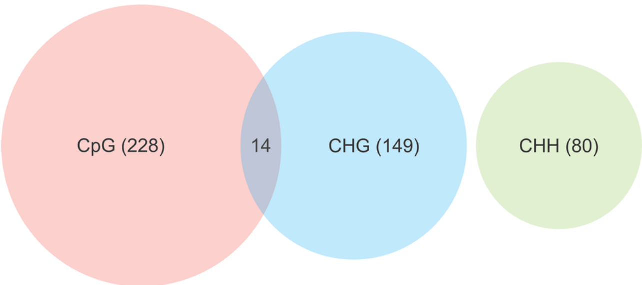

PPL_13777_Figure_7.tif

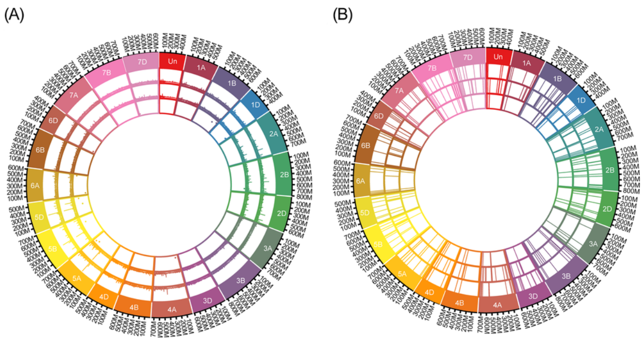

PPL_13777_Figure_8.tif

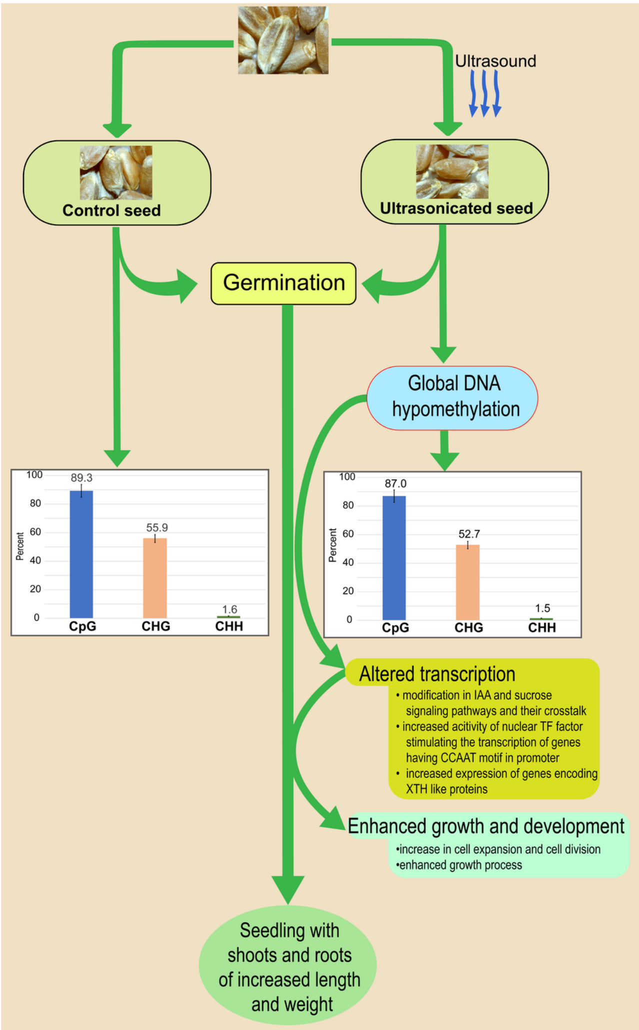

PPL_13777_Figure_9.tif

Table 1. Significantly up- or down-regulated DEGs and related metabolic and cellular functions. Negative values indicate down-regulation; positive values indicate up-regulation in response to the ultrasonication of winter wheat seeds

DEG ID	Up/down regulation	Protein (Pathway)
TraesCS1B02G317500	4.69	starch synthase (Starch biosynthesis)
TraesCS1B02G433300	5.79	starch synthase (Starch biosynthesis)
TraesCS1D02G027300	3.13	subtilisin-chymotrypsin inhibitor-2B-like *
TraesCS1D02G375100	4.45	starch synthase (Starch biosynthesis)
TraesCS1D02G411300	2.81	starch synthase (Starch biosynthesis)
TraesCS2B02G510200	4.45	xyloglucan endotransglucosylase/hydrolase protein 9-like isoform X2 *
TraesCS4A02G081000	5.27	amydase (IAA biosynthesis VI (via indole-3-acetamide))
TraesCS5A02G350600	2.28	SCS dimer (TCA cycle (plant)); Photosynthesis - antenna proteins (Lhcb1)
TraesCS5A02G454200	6.18	starch synthase (Starch biosynthesis)
TraesCS5A02G454300	5.11	starch synthase (Starch biosynthesis)
TraesCS5B02G353200	2.75	SCS dimer (TCA cycle (plant))
TraesCS5D02G227000	-4.22	low molecular mass early light-inducible protein HV90, chloroplastic-like *
TraesCS5D02G227500	-4.23	low molecular mass early light-inducible protein HV90, chloroplastic-like *
TraesCS5D02G464700	4.01	starch synthase (Starch biosynthesis)
TraesCS6A02G093700	3.79	starch synthase (Starch biosynthesis)
TraesCS6A02G350300	-3.71	cold-shock protein CS120-like (dehydrin) *
TraesCS6D02G088800	3.44	starch synthase (Starch biosynthesis)
TraesCS7D02G057200	8.57	uncharacterized isomerase BH0283-like *
*: description based on NCBI, otherwise on Plant Reactome and KEGG mapping		

Table 2. Distribution of DMGs in upstream, overlapping and downstream regions based on the GO annotation results.

	CpG context			CHG context			CHH context		
	Upstream	Overlapping	Downstream	Upstream	Overlapping	Downstream	Upstream	Overlapping	Downstream
Biological process	16 ↑ 24↓	17 ↑ 70 ↓	34 ↑ 25 ↓	29 ↑ 31 ↓	32↑ 59 ↓	17 ↑ 24 ↓	15 ↑ 9 ↓	12 ↑ 18 ↓	10 ↑ 18↓
Molecular function	7 ↑ 16 ↓	13 ↑ 32 ↓	9 ↑ 11 ↓	12 ↑ 13 ↓	16↑ 13 ↓	7 ↑ 7 ↓	3 ↑ 9↓	2 ↑ 10 ↓	5 ↑ 8 ↓
Cellular component	5 ↑ 21 ↓	12 ↑ 65 ↓	13 ↑ 22 ↓	6 ↑ 10 ↓	16 ↑ 31 ↓	8 ↑ 8 ↓	3 ↑ 12 ↓	2 ↑ 9 ↓	4 ↑ 12 ↓

Table 3. Participation of the DMGs in different pathways based on Plant Reactome and KEGG mapping. DMGs are presented according to the contexts and regions in which they were methylated differentially in 7-day-old seedlings after seed ultrasonication. Numbers mean the number of sequences involved; ↑ indicates hypermethylation while ↓ indicates hypomethylation compared to non-ultrasonicated samples. Note: A sequence can be involved in multiple pathways and a sequence may occur more than once in the table if it has been methylated differently in multiple contexts or regions.

Pathway groups	CpG			CHG			CHH		
	upstream	overlapping	downstream	upstream	overlapping	downstream	upstream	overlapping	downstream
I. Cellular processes and energy and precursor metabolism									
- Protein metabolism: Translation		1↑ 1↓			2↑	1↓		1↓	1↑ 1↓
- Cell cycle (mitosis)		1↑ 1↓		2↑	1↑	1↑			2↑
- Photosynthesis	1↓	1↓	1↓		1↓	1↓			
- TCA cycle		1↓			1↑ 1↓			1↓	
- Oxidative phosphorylation		1↑ 6↓	2↓		1↓	1↓	1↓		
- Nucleocytoplasmic transport		1↑							
- RNA degradation					1↑				
- Protein export					1↓				
II. Growth and developmental processes	1↑ 4↓	7↑ 5↓	5↑ 1↓	4↓	1↑ 3↓		1↑	3↓	1↑ 1↓
III. Metabolism and regulation									
- Amino acid metabolism	4↑ 5↓	9↓	4↑ 8↓	5↑ 8↓	8↑ 4↓	6↓	8↓	3↑ 1↓	5↓
- Carbohydrate metabolism	5↓	1↑ 7↓	3↑ 1↓	5↑ 6↓	4↑ 5↓	1↓	3↓	1↓	3↓
- Cofactor biosynthesis	1↑ 5↓	6↑ 11↓	2↓	2↑ 2↓	1↑ 12↓	2↑ 2↓	2↓	3↓	4↓
- Detoxification		1↑		1↑	1↑				
- Hormone signaling, transport and metabolism	3↑ 1↓	5↑ 12↓	6↑ 10↓	3↑ 1↓	2↑ 3↓	2↑ 2↓	1↑ 6↓	2↓	1↑ 4↓

- Secondary metabolism	2↑	3↑ 3↓	2↓	4↑ 5↓	3↑ 1↓	1↓	3↑ 5↓		7↓
- Fatty acid and lipid metabolism	2↓	1↓		6↓	4↓	1↑			3↓
- Inorganic nutrients metabolism			1↓		1↑				
- Nucleotide metabolism					2↑ 2↓	1↑			
- Photorespiration	1↑	2↓			1↓				
- Glycerophospholipid metabolism	3↑	3↓							
- Xenobiotics metabolism			2↓		3↑		3↓		
- Glycan biosynthesis and metabolism								4↓	
IV. Response to stimuli: abiotic stimuli and stresses		4↑ 12↓	5↓			3↓	3↓		6↑ 5↓
V. Response to stimuli: biotic stimuli and stresses	1↑ 1↓	2↑		1↑	2↓	1↓			1↑
VI. Circadian rhythm	1↑			1↓					